Inverse Reconstruction of Unsteady Aerodynamic Loads Acting on Railway Vehicles

SHUO HAO, SU-MEI WANG, ZHENG-WEI CHEN,
WEI-JIA ZHANG and YI-QING NI

ABSTRACT

During normal operation, railway vehicles often endure significant vibrations due to unsteady aerodynamic loads. Precisely quantifying these transient forces offers essential insights for operational safety monitoring and vehicle aerodynamic testing. In this paper, we introduce an innovative inverse method for reconstructing active aerodynamic loads using a limited number of acceleration measurements. This method capitalizes on health monitoring instruments already present on the vehicles, thereby eliminating the necessity for supplementary pressure sensors on the vehicle's exterior surface, as mandated by traditional direct pressure measurement strategies. We develop a Multi-Task Gaussian Processes (MTGP) inverse estimation technique to calculate the conditional probability distribution of loads given the noise-affected acceleration data. The MTGP approach boasts the advantage of analytically forming the posterior of unsteady aerodynamic loads at any time point, as well as offering high reconstruction accuracy. To validate our proposed method, we utilize a numerical example with a 31 DOF railway vehicle model. Aerodynamic loads generated by two trains passing each other are applied to the vehicle model, and acceleration data from the bogies are employed for the inverse reconstruction process. Our results successfully demonstrate the feasibility of reconstructing unsteady aerodynamic loads on railway vehicles, highlighting the potential of our novel approach.

INTRODUCTION

Railway vehicles are subject to various external forces during operation, among which unsteady aerodynamic loads play a critical role in influencing the vehicle's dynamic behavior, stability, and safety, which might occur in several scenarios, such as two vehicles passing each other [1], a single train moving through a double-track tunnel [2], as well as the local landforms induced crosswinds [3]. The accurate quantification of these loads is essential for the development and optimization of railway vehicle designs,

Shuo HAO, PhD Candidate, Email: cee-shuo.hao@connect.polyu.hk. National Rail Transit Electrification and Automation Engineering Technology Research Center (Hong Kong Branch), Department of Civil and Environmental Engineering, The Hong Kong Polytechnic University, Hung Hom, Kowloon, Hong Kong

as well as for monitoring their performance in operational conditions. Despite its importance, the inverse reconstruction of unsteady aerodynamic loads acting on railway vehicles remains a challenging problem due to the complexity of the underlying fluid-structure interactions and the limitations of traditional measurement techniques. Existing approaches for quantifying aerodynamic loads often rely on the direct deployment of multiple pressure sensors on the vehicle's surface [4]. While these methods provide valuable insights into the local pressure distribution, they may be insufficient for capturing the global load characteristics and may impose significant logistical and economic burdens. Consequently, there is a pressing need to explore alternative strategies that can overcome these limitations and facilitate a more accurate, efficient, and cost-effective assessment of unsteady aerodynamic loads on railway vehicles.

In this paper, we address this challenge by proposing a novel inverse reconstruction strategy for estimating active aerodynamic loads using a limited number of acceleration measurements. The strategy circumvents the need for extensive sensor arrays and offers a more streamlined and reliable means of determining the unsteady aerodynamic loads acting on railway vehicles. By leveraging the developed Multi-Task Gaussian Processes (MTGP) method, we are able to estimate the posterior distribution of aerodynamic loads taking into consideration the noise of measurements.

Through a comprehensive series of theoretical analyses and numerical simulations, we demonstrate the feasibility and efficacy of our proposed method in accurately reconstructing unsteady aerodynamic loads. Our findings not only highlight the potential of this innovative approach as a valuable tool for railway vehicle design and performance assessment but also pave the way for future research aimed at advancing the state of the art in unsteady aerodynamic load quantification and its practical applications.

THEORETICAL BACKGROUND

The railway vehicle under normal operating conditions could be modeled as a linear discrete-time dynamical system. Under the action of unsteady aerodynamic loads, the vehicle's response at the k-th time step can be formulated using the weighting sequence description shown in Eq. 1, given that the vehicle is of zero initial condition at 0-th time step [5].

$$\boldsymbol{y}_k = \sum_{i=0}^{k} \mathbf{H}_i \boldsymbol{f}_{k-i} \tag{1}$$

in which $\boldsymbol{y}_k \in \mathbb{R}^{n_s}$ is the measurement at k-th time step; $\mathbf{H}_i \in \mathbb{R}^{n_s \times n_f}$ is the system Markov parameters that could either be calculated using mechanical parameters or modal properties; $\boldsymbol{f}_{k-i} \in \mathbb{R}^{n_f}$ is the input force sequence. Here the n_s and n_f refer to the number of sensors and forces, respectively. The weighting sequence description illustrates the system response at each time step caused by all previous force history. In practice, the structural responses are measured at equally spaced time steps. By denoting n_t as the total number of time steps, there are n_t equations that can be drawn from Eq.

1, that is

$$\begin{bmatrix} \boldsymbol{y}_0 \\ \boldsymbol{y}_1 \\ \vdots \\ \boldsymbol{y}_{n_t-1} \end{bmatrix} = \begin{bmatrix} \mathbf{H}_0 & \mathbf{0} & \cdots & \mathbf{0} \\ \mathbf{H}_1 & \mathbf{H}_0 & & \vdots \\ \vdots & \vdots & \ddots & \mathbf{0} \\ \mathbf{H}_{n_t-1} & \mathbf{H}_{n_t-2} & \cdots & \mathbf{H}_0 \end{bmatrix} \begin{bmatrix} \boldsymbol{f}_0 \\ \boldsymbol{f}_1 \\ \vdots \\ \boldsymbol{f}_{n_t-1} \end{bmatrix} \tag{2}$$

In this paper, we use $\hat{\boldsymbol{y}}, \mathbf{H}, \boldsymbol{f}$ to represent the full vectors/matrix shown in Eq. 2, and denote $\boldsymbol{y}$ as the observation on $\hat{\boldsymbol{y}}$. The aerodynamic load reconstruction problem for railway vehicles can be stated as follows: given $\boldsymbol{y}$ and $\mathbf{H}$, compute $\boldsymbol{f}$. Although Eq. 2 incorporates the complete physical information of the system, this problem is generally ill-posed. In most cases, the $\mathbf{H}$ matrix is singular and cannot be directly inverted to compute the inverse of $\boldsymbol{f}$. The solution set for Eq. 2 is an infinite set, which can be regarded as a polyhedron formed by the intersection of several hyperplanes. In other instances, even when the $\mathbf{H}$ matrix is non-singular, small measurement errors in response measurements $\hat{\boldsymbol{y}}$ can lead to significant errors in the computed forces.

To address this issue, we propose a novel MTGP method for the vehicle aerodynamic load reconstruction problem. This method computes the analytical posterior distribution of force histories given the measured acceleration data, i.e., $p(\boldsymbol{f}|\boldsymbol{y})$. MTGP is formulated within the Bayesian framework and can be considered a novel Bayesian regularization technique [6]. The prior assumption in MTGP is that all forces are independent Gaussian Processes, with their mean and covariance functions assumed to be 0 and parameterized positive definite kernel functions, that is,

$$f(t) \sim \mathcal{GP}(0, k_i(t, t')), i = 1, 2, \cdots, n_f \tag{3}$$

According to Eq. 2, the force vector on the right side of the equation consists of jointly correlated Gaussian variables, while the left side represents acceleration values that can be expressed by the linear combination of these Gaussian variables. Assuming that the measurement noise is Gaussian white noise, any finite set of measured acceleration data will also follow a multivariate Gaussian distribution. MTGP constructs the joint distribution of all Gaussian variables, including those related to force and measured acceleration. The posterior distribution $p(\boldsymbol{f}|\boldsymbol{y})$, according to Gaussian Processes regression theory, is another multivariate Gaussian distribution, for which the mean and covariance can be analytically derived.

The multivariate Gaussian distribution among all force variables is first defined as

$$\boldsymbol{f} \sim (\mathbf{0}, \mathbf{\Sigma}_{ff}) \tag{4}$$

with

$$\mathbf{\Sigma}_{ff} = \text{diag}\left[\mathbf{\Sigma}_1, \mathbf{\Sigma}_2, \cdots \mathbf{\Sigma}_{n_f}\right] \tag{5}$$

where $\mathbf{\Sigma}_i, i = 1, 2, \cdots, n_f$ are respectively drawn based on the covariance functions $k_i(t, t')$. Then, we consider that the measured acceleration data differs from the function values $\boldsymbol{y}$ by additive noise. We further assume that noise contamination of acceleration data from any single sensor preserves homogeneity. That is, we have

$$\boldsymbol{y} = \mathbf{H}\boldsymbol{f} + \boldsymbol{w} \tag{6}$$

with

$$\boldsymbol{w} = [\boldsymbol{w}_1; \boldsymbol{w}_2; \cdots; \boldsymbol{w}_{n_s}] \tag{7}$$

The vectors $\boldsymbol{w}_1, \boldsymbol{w}_2, \cdots, \boldsymbol{w}_{n_s}$ contain variables drawn from n_s independent identically distributed Gaussian distribution, of which mean values are equal to zero and standard deviations equal to $\sigma_1, \sigma_2, \cdots, \sigma_{n_s}$. Therefore, $\boldsymbol{w}$ follows multivariate Gaussian distribution. The mean vector of the distribution $\mathbb{E}(\boldsymbol{w})$ is $\mathbf{0}$, and the covariance matrix $\mathbb{E}(\boldsymbol{w}\boldsymbol{w}^\top)$ is denoted by $\boldsymbol{\Psi}$, which is given by

$$\boldsymbol{\Psi} = \text{diag}\left[\sigma_1^2\mathbf{I}, \sigma_2^2\mathbf{I} \cdots \sigma_{n_s}^2\mathbf{I}\right] \tag{8}$$

Having the mean and covariance of $\boldsymbol{f}$ and $\boldsymbol{w}$, the multivariate Gaussian distribution of $\boldsymbol{y}$ could be formulated, that is

$$\mathbb{E}(\boldsymbol{y}) = \mathbb{E}(\boldsymbol{H}\boldsymbol{f} + \boldsymbol{w}) = \mathbf{H}\mathbb{E}(\boldsymbol{f}) + \mathbb{E}(\boldsymbol{w}) = \mathbf{0} \tag{9}$$

$$\begin{aligned}\boldsymbol{\Sigma}_{yy} = \mathbb{E}(\boldsymbol{y}\boldsymbol{y}^\top) &= \mathbb{E}(\boldsymbol{H}\boldsymbol{f}\boldsymbol{f}^\top\mathbf{H}^\top + \boldsymbol{w}\boldsymbol{w}^\top) \\ &= \mathbf{H}\mathbb{E}(\boldsymbol{f}\boldsymbol{f}^\top)\mathbf{H}^\top + \mathbb{E}(\boldsymbol{w}\boldsymbol{w}^\top) \\ &= \mathbf{H}\boldsymbol{\Sigma}_{ff}\mathbf{H}^\top + \boldsymbol{\Psi}\end{aligned} \tag{10}$$

Correspondingly, the covariance matrices that contain the covariance between variables from forces and measurements can be written as

$$\boldsymbol{\Sigma}_{fy} = \boldsymbol{\Sigma}_{yf}^\top = \mathbb{E}(\boldsymbol{f}\boldsymbol{y}^\top) = \mathbb{E}(\boldsymbol{f}\boldsymbol{f}^\top\mathbf{H}^\top) = \boldsymbol{\Sigma}_{ff}\mathbf{H}^\top \tag{11}$$

Hence, the multivariate Gaussian distribution involving force and measured acceleration could be constructed

$$\begin{bmatrix}\boldsymbol{f} \\ \boldsymbol{y}\end{bmatrix} \sim \mathcal{N}\left(\mathbf{0}, \begin{bmatrix}\boldsymbol{\Sigma}_{ff} & \boldsymbol{\Sigma}_{fy} \\ \boldsymbol{\Sigma}_{yf} & \boldsymbol{\Sigma}_{yy}\end{bmatrix}\right) \tag{12}$$

The MTGP aims to compute the posterior distribution of forces given measured acceleration data, that is, $p(\boldsymbol{f}|\boldsymbol{y})$, which could be formulated using the Bayes' theorem

$$p(\boldsymbol{f}|\boldsymbol{y};\boldsymbol{\theta}) = \frac{p(\boldsymbol{f}, \boldsymbol{y}; \boldsymbol{\theta})}{\int p(\boldsymbol{f}, \boldsymbol{y}; \boldsymbol{\theta})\mathrm{d}\boldsymbol{f}} \tag{13}$$

where $\boldsymbol{\theta}$ refers to the hyperparameters that include parameters in the covariance function as well as the σ_i for noise stand deviation. The probability density function in the numerator is easily derived since $\boldsymbol{f}$ and $\boldsymbol{y}$ jointly follow multivariate Gaussian distribution shown in Eq. 12, which is

$$p(\boldsymbol{f}, \boldsymbol{y}; \boldsymbol{\theta}) = \frac{1}{(2\pi)^{n_t n_f + n_t n_s}|\hat{\boldsymbol{\Sigma}}|^{\frac{1}{2}}} \exp\left(-\frac{1}{2}\begin{bmatrix}\boldsymbol{f} \\ \boldsymbol{y}\end{bmatrix}^\top \hat{\boldsymbol{\Sigma}}^{-1}\begin{bmatrix}\boldsymbol{f} \\ \boldsymbol{y}\end{bmatrix}\right) \tag{14}$$

where $\hat{\boldsymbol{\Sigma}}$ represents the full covariance matrix in Eq. 12. Given that the denominators in Eq. 13 and 14 are both proportionality constants that do not depend on $\boldsymbol{f}$, as well as the inverse of $\hat{\boldsymbol{\Sigma}}$ could be expressed by corresponding submatrices, i.e., $\boldsymbol{\Sigma}_{ff}, \boldsymbol{\Sigma}_{fy}, \boldsymbol{\Sigma}_{yf}$, and $\boldsymbol{\Sigma}_{yy}$. The posterior distribution in Eq. 13 is equivalent to another multivariate Gaussian distribution

$$p(\boldsymbol{f}|\boldsymbol{y};\boldsymbol{\theta}) = \frac{1}{z}\exp\left(-\frac{1}{2}[\boldsymbol{f} - \bar{\boldsymbol{f}}]^\top \text{cov}(\boldsymbol{f})^{-1}[\boldsymbol{f} - \bar{\boldsymbol{f}}]\right) \tag{15}$$

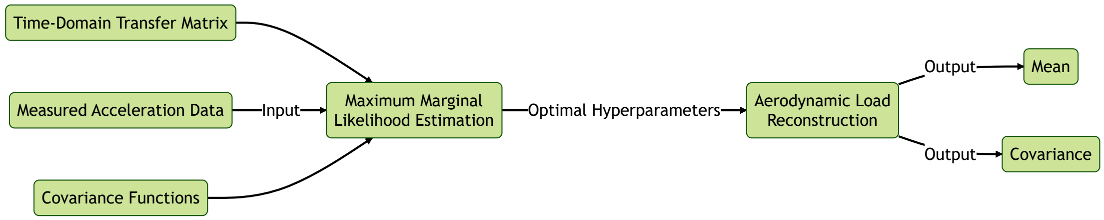

Figure 1. MTGP working flowchart for computation of aerodynamic load.

where z is a constant that is associated with hyperparameters; the posterior mean vector $\bar{\boldsymbol{f}}$ and covariance matrix $\mathrm{cov}(\boldsymbol{f})$ are respectively given by

$$\bar{\boldsymbol{f}} = \boldsymbol{\Sigma}_{fy}\boldsymbol{\Sigma}_{yy}^{-1}\boldsymbol{y} \tag{16}$$

$$\mathrm{cov}(\boldsymbol{f}) = \boldsymbol{\Sigma}_{ff} - \boldsymbol{\Sigma}_{fy}\boldsymbol{\Sigma}_{yy}^{-1}\boldsymbol{\Sigma}_{yf} \tag{17}$$

The hyper-parameters could be optimized using the maximum marginal likelihood method, in which the marginal likelihood refers to the denominator in Eq. 13. Moreover, as a compelling property of Gaussian Processes, the analytical expression for marginal likelihood and its derivative is easily formulated. Hence, a gradient-based optimization algorithm (e.g., L-BFGS) is selected for the maximum marginal likelihood in the aerodynamic load reconstruction process. With the optimized hyperparameters, one could directly compute the posterior distribution of forces with Eq. 16 and 17.

A flowchart is summarized in Fig. 1 for the MTGP method, based on which we will be able to conduct the unsteady aerodynamic load reconstruction.

RAILWAY VEHICLE MODEL DESCRIPTION

The full railway vehicle model constructed in this paper is schematically shown in Fig. 2, which consists of a car body, two bogies, and four wheel-sets. The bogies and car body exhibit five types of motion (lateral, vertical, roll, yaw, and pitch), while the wheel-sets have four (lateral, vertical, roll, and yaw). The model is built based on the following assumptions: (i) the vehicle is modeled as an assemblage of rigid bodies connected by primary and secondary suspensions; (ii) the vehicle runs on a constant forward velocity and the longitudinal (x-direction) motions of all rigid bodies are neglected; (iii) all amplitudes of the motions for the system components remain small, and thus the linear elastic theory applies; and (iv) the wheel-sets are linearly connected with the substructures. The equation of motion of the train is formulated based on the Lagrangian principle. Mass and stiffness matrices $\mathbf{M}, \mathbf{K}$ can be obtained accordingly via the Euler-Lagrange equation, that is

$$\frac{\mathrm{d}}{\mathrm{d}t}\frac{\partial L}{\partial \dot{\boldsymbol{x}}} - \frac{\partial L}{\partial \boldsymbol{x}} = \mathbf{0} \tag{18}$$

where $\boldsymbol{x}, \dot{\boldsymbol{x}} \in \mathbb{R}^{31}$ is the vector that includes all displacements and velocities of rigid bodies in the system; L is the Lagrangian identity that could be formulated as the difference between kinetic energy and potential energy. Due to space limitations, the detailed expressions of energies are eliminated. The damping matrix $\mathbf{C}$ is generated based on a similar form of the stiffness matrix $\mathbf{K}$.

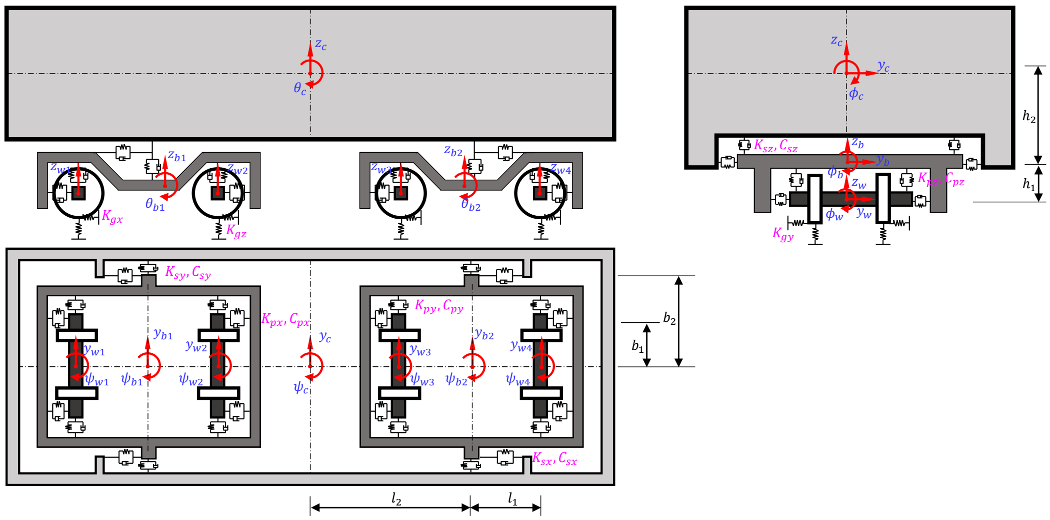

Figure 2. Schematic diagram of 31-DOF railway vehicle model.

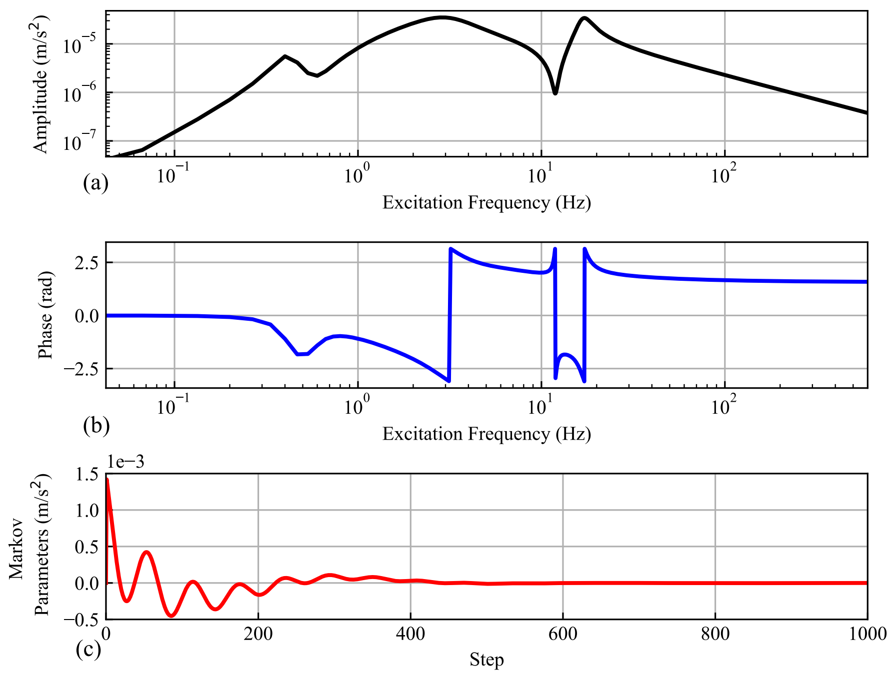

Figure 3. Frequency response function and Markov parameters between y_c and y_{b1}.

The frequency response function concerning any two DOFs could be calculated using the formulated mass, damping, and stiffness matrices. Furthermore, the corresponding Markov parameters can be computed using inverse Fourier transformation on the frequency response functions, which would be used to construct the time-domain transfer matrix $\mathbf{H}$ in Eq. 2. Fig. 3 shows an instance of the frequency response function and Markov parameters between y_c and y_{b1}. In practice, these modal properties could be directly measured through experimental modal analysis without any prior specification over the vehicle model [7].

ANALYTICAL TEST CASE

In this section, we consider the scenario where two individual railway vehicles pass each other in an open-air environment. We leverage the simulation results from the study on transient pressure on vehicle surfaces by Huang et al. [1], which provides the pressure time history for a single spatial point located at the center of the vehicle's body. Notably, significant fluctuations occur as the front and rear ends of the railway vehicle pass this point.

We assume constant pressure along the vertical direction at each time step, while the pressure in the longitudinal direction varies with time. Fig. 4 (a) illustrates the transient pressure for each time step and vertical longitudinal coordinate. Next, we manually convert the pressure at each time step into lateral force and yaw moment acting on the vehicle body, as depicted in Fig. 4 (b).

To compute the railway vehicle dynamical system response, we employ the 4$^{\text{th}}$ order Runge-Kutta method. We assume that the lateral and yaw acceleration of the two bogies

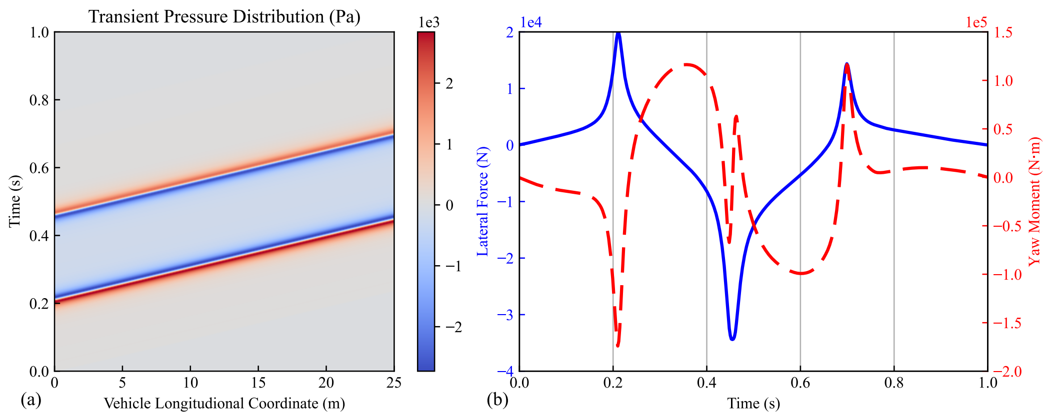

Figure 4. Transient pressure distribution and equivalent lateral force and yaw moment acting on the vehicle body.

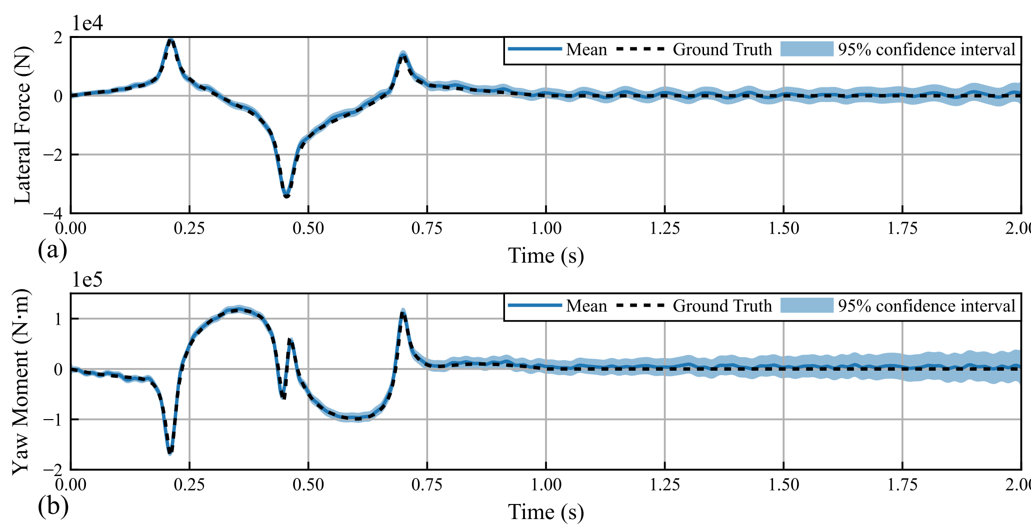

Figure 5. Reconstructed lateral force and yaw moment using MTGP.

under aerodynamic load is available, with a sampling frequency of 750 Hz. Gaussian white noise with a variance of 10^{-2} is added to the raw data. It is important to note that the yaw motions of the two bogies are identical during the passing process; thus, only $y_{b1}, \psi_{b1}, y_{b2}$ will be used for load reconstruction.

The MTGP method is then applied to reconstruct the lateral force and yaw moment based on the flowchart in Fig. 1. The time-domain transfer matrix is constructed using the modal parameters, with the measured acceleration data being the noise-contaminated $y_{b1}, \psi_{b1}, y_{b2}$. Gaussian kernel functions serve as the covariance functions for both lateral force and yaw moment. The resulting output is the posterior distribution of the aerodynamic forces, a multivariate Gaussian distribution as demonstrated in Eq. 15. Fig. 5 reveals that the ground truths of lateral force and yaw moment fall within the 95% confidence interval, successfully showcasing the applicability of MTGP in reconstructing unsteady aerodynamic loads acting on railway vehicles.

CONCLUDING REMARKS

In this paper, we introduce a pioneering approach for quantifying unsteady aerodynamic forces exerted on railway vehicles, utilizing acquired acceleration data. Furthermore, we present an innovative technique, MTGP, to address the ill-posed nature of the reconstruction process, allowing for the consideration of measurement noise and enhancing the precision of the reconstructed outcomes. As high-speed railway technology advances and demands for operational safety increase, this innovative method holds promise for its application in future railway vehicle aerodynamic testing and structural operational safety monitoring systems.

REFERENCES

1. Huang, S., Z. W. Li, and M. Z. Yang. 2019. "Aerodynamics of high-speed maglev trains passing each other in open air," *Journal of Wind Engineering & Industrial Aerodynamics*, 188:151–160.
2. Liu, T. H., Z. W. Chen, X. D. Chen, T. Z. Xie, and J. Zhang. 2017. "Transient loads and their influence on the dynamic responses of trains in a tunnel," *Tunnelling and Underground Space Technology*, 66:121–133.
3. Chen, Z. W., T. H. Liu, M. Li, M. Yu, Z. J. Lu, and D. R. Liu. 2019. "Dynamic response of railway vehicles under unsteady aerodynamic forces caused by local landforms," *Wind and Structures*, 29:149–161.
4. Baker, C., S. Jordan, T. Gilbert, A. Quinn, M. Sterling, T. Johnson, and J. Lane. 2014. "Transient aerodynamic pressures and forces on trackside and overhead structures due to passing trains. Part 1: Model-scale experiments; Part 2: Standards applications," *Proceedings of the Institution of Mechanical Engineers, Part F: Journal of Rail and Rapid Transit*, 228:37–70.
5. Sanchez, J. and H. Benaroya. 2014. "Review of force reconstruction techniques," *Journal of Sound and Vibration*, 333:2999–3018.
6. Barber, D. 2012. *Bayesian reasoning and machine learning*, Cambridge University Press.
7. Luo, Y. K., L. Zhou, and Y. Ni. 2022. "Towards the understanding of wheel-rail flange squeal: In-situ experiment and genuine 3D profile-enhanced transient modelling," *Mechanical Systems and Signal Processing*, 180:109455.